Structure
Article

Structural Basis for EGF Receptor Inhibition by the Therapeutic Antibody IMC-11F8

Shiqing Li,[1,3] Paul Kussie,[2] and Kathryn M. Ferguson[1,*]
[1]Department of Physiology, University of Pennsylvania School of Medicine, Philadelphia, PA 19104, USA
[2]Protein Science Department, ImClone Systems, New York, NY 10014, USA
[3]Present address: Blank Rome LLP, One Logan Square, Philadelphia, PA 19103, USA.
*Correspondence: ferguso2@mail.med.upenn.edu
DOI 10.1016/j.str.2007.11.009

SUMMARY

Therapeutic anticancer strategies that target and inactivate the epidermal growth factor receptor (EGFR) are under intense study in the clinic. Here we describe the mechanism of EGFR inhibition by an antibody drug IMC-11F8. IMC-11F8 is a fully human antibody that has similar antitumor potency as the chimeric cetuximab/Erbitux and might represent a safer therapeutic alternative. We report the X-ray crystal structure of the Fab fragment of IMC-11F8 (Fab11F8) in complex with the entire extracellular region and with isolated domain III of EGFR. We compare this to our previous study of the cetuximab/EGFR interaction. Fab11F8 interacts with a remarkably similar epitope, but through a completely different set of interactions. Both the similarities and differences in binding of these two antibodies have important implications for the development of inhibitors that could exploit this same mechanism of EGFR inhibition.

INTRODUCTION

The epidermal growth factor receptor (EGFR) is the target of several current and developing anticancer therapies, including monoclonal antibodies directed against the extracellular region of the receptor and small-molecule inhibitors of the intracellular tyrosine kinase domain (Marshall, 2006; Scaltriti and Baselga, 2006). In fact, the EGF receptor was the first cell-surface receptor to be associated directly with human cancers (Todaro et al., 1976). We have been interested in understanding the structural basis of EGFR inhibition by antibodies against the extracellular region, both to enhance our understanding of the normal mechanisms of receptor activation and to gain insight into how to develop improved therapeutic agents.

The first step in normal EGFR activation is ligand-induced receptor dimerization (Schlessinger, 2000), which brings two intracellular kinase domains together that become activated allosterically (Zhang et al., 2006). Structural snapshots of the ligand-induced dimerization process have been provided by X-ray crystallographic studies of the extracellular regions of EGFR (Ferguson et al., 2003; Garrett et al., 2002; Ogiso et al., 2002) and the other three members of the EGFR/ErbB family of RTKs, namely ErbB2/HER2/Neu (Cho et al., 2003; Franklin et al., 2004; Garrett et al., 2003), ErbB3/HER3 (Cho and Leahy, 2002), and ErbB4/HER4 (Bouyain et al., 2005). The unliganded extracellular regions of EGFR, ErbB3, and ErbB4 all adopt a characteristic "tethered" conformation (Bouyain et al., 2005; Cho and Leahy, 2002; Ferguson et al., 2003) in which the primary receptor dimerization site is occluded by intramolecular interactions between two cysteine-rich domains (domains II and IV). Upon ligand binding, the receptor undergoes a dramatic domain rearrangement (Burgess et al., 2003) in addition to more local ligand-induced conformational changes (Dawson et al., 2005) that serve to expose and optimize the receptor dimerization site. As shown in Figure 1, a single EGF molecule binds simultaneously to both domains I and III of the EGFR extracellular region, forcing it to adopt the extended configuration that is capable of domain II-mediated dimerization (Burgess et al., 2003).

This structural model for ligand-induced EGFR dimerization suggests several possible approaches for inhibition, some of which are exploited by therapeutic antibodies that have emerged from early screens (Ferguson, 2004). For example, the chimeric cetuximab (Erbitux) antibody inhibits EGFR activation by competing directly with EGF for its binding site on domain III of the receptor (Li et al., 2005). Cetuximab binding also sterically impedes adoption of the extended configuration. On the other hand, the anti-ErbB2 antibody pertuzumab binds directly to the presumed domain II (hetero)dimerization site of ErbB2 (Franklin et al., 2004), and the anti-EGFR antibody mAb806 binds to a domain II epitope close to the receptor's dimerization site (Johns et al., 2004).

In an effort to generate fully human anti-EGFR antibodies that inhibit the receptor, a nonimmunized human Fab phage display library containing 3.7×10^{10} unique clones (de Haard et al., 1999; Lu et al., 2004b) was screened for Fab fragments that would bind A431 epidermoid carcinoma cells (which express high levels of EGFR) (Lu et al., 2004b) and also compete with cetuximab for binding to the cell surface (Liu et al., 2004). Of four unique Fab clones that were selected, only one (termed 11F8) displayed a dose-dependent inhibitory effect on EGF-stimulated EGFR activation in A431 cells (Liu et al., 2004). A fully human antibody bearing 11F8 antigen-combining regions (IMC-11F8) inhibits EGFR activation in several cell lines (Liu et al., 2004; Lu et al., 2004b), blocks tumor growth in xenograft models (Lu et al., 2005; Prewett et al., 2004), and has performed well in phase I clinical trials (Kuenen et al., 2006). As a fully human antibody, IMC-11F8 has a significant advantage over the chimeric cetuximab antibody, which contains entirely mouse-derived

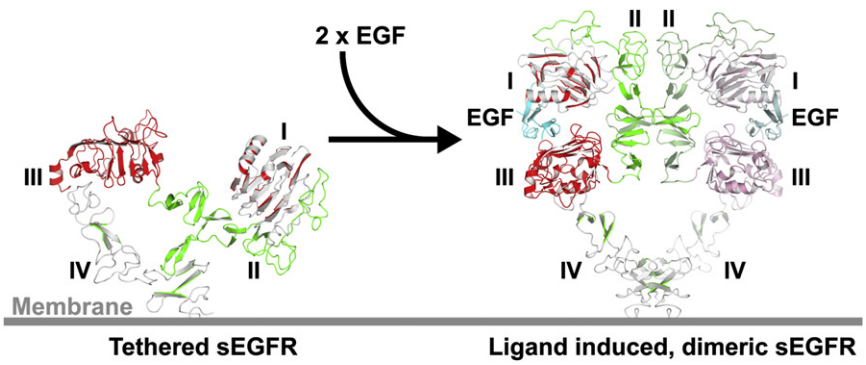

Figure 1. Ligand-Induced Dimerization of EGFR

In the unliganded state, EGFR exists as a tethered monomer (left). Domain II (green) interacts with domain IV (white, with secondary structure highlighted in green); domains I (white with red highlights) and III (red) are far apart. The arrangement of the domains in the ligand-induced, dimeric state (right) is dramatically different. Domains I and III are closer together and interact with the ligand (EGF, cyan). The colors of the right-hand molecule in the dimer are lightened for contrast. Domain IV in the dimer is modeled as described (Ferguson et al., 2003). The gray line represents the approximate location of the membrane. This figure uses coordinates from PDB ID codes 1YY9, 1NQL, and 1IVO.

sequences in its variable domains that are fused to human constant domains. Cetuximab, which is approved for use in advanced colorectal cancer and head and neck squamous-cell carcinoma, elicits immune reactions in ~19% of cases (Lenz, 2007) (Erbitux [cetuximab], package insert, ImClone Systems, New York and Bristol-Myers Squibb, Princeton, NJ, 2006). As expected for a fully human antibody (Weiner, 2006), IMC-11F8 has shown no evidence of such immune hypersensitivity in clinical trials (Kuenen et al., 2006).

To establish the mechanism of EGFR inhibition by this fully human therapeutic antibody, we determined the X-ray crystal structure of the Fab fragment of IMC-11F8 bound to the EGFR extracellular region. IMC-11F8 recognizes a remarkably similar EGFR epitope to that previously described for cetuximab (Li et al., 2005), and these two antibodies likely share a similar mode of EGFR inhibition. The details of the antibody/receptor interactions are, however, quite different. We discuss features of the EGFR epitope recognized by these two antibodies that are likely to make it well suited for this type of molecular interaction.

RESULTS AND DISCUSSION

IMC-11F8 Binds to the EGF-Binding Site of EGFR

To understand how IMC-11F8 inhibits EGF activation of EGFR, we analyzed its binding to the isolated EGFR extracellular region and sought to determine the structural basis for its EGFR recognition. We generated the antigen-binding Fab fragment of IMC-11F8 (Fab11F8) by papain digestion of the IgG protein. The EGFR extracellular region (sEGFR) was produced in insect cells as described (Ferguson et al., 2000).

Using surface plasmon resonance (SPR), we analyzed sEGFR binding to Fab11F8 that had been immobilized on a CM5 biosensor chip. As shown in Figure 2A, sEGFR binds strongly to Fab11F8, with a K_D value of 3.3 ± 0.5 nM, similar to values reported previously for the binding of an scFv comprising the V_L and V_H domains of IMC-11F8 to immobilized sEGFR (Lu et al., 2004a). This compares well with the K_D value of 2.3 ± 0.5 nM for the cetuximab Fab binding to sEGFR (Li et al., 2005). To examine the ability of Fab11F8 to block EGF binding by sEGFR, we used SPR to monitor the association of sEGFR (600 nM) with immobilized EGF in the presence of increasing concentrations of Fab11F8. Fab11F8 efficiently impaired EGF binding by sEGFR, which fell to almost zero upon addition of one molar equivalent of the Fab fragment (Figure 2B).

Crystal Structure of a Fab11F8/sEGFR Complex

Crystals of a purified Fab11F8/sEGFR complex that diffracted to 3.3 Å resolution were obtained, and the structure was solved using molecular replacement (MR) methods. Domain III of sEGFR and a homology model for the Fab were placed in the Fab11F8/sEGFR structure using the program MOLREP (Vagin and Teplyakov, 1997), and used to calculate starting phases. Following several rounds of model building and refinement, significant additional density could be seen for the majority of domain IV and the region of domain II that extends from domain III to the domain II/IV intramolecular tether interaction. Even with this improved model, an MR solution for domain I could not be identified. No interpretable density could be discerned for the remainder of domain II or any of domain I in composite simulated annealing (SA) omit maps calculated using CNS (Brunger et al., 1998), or in density modified maps with reduced phase bias calculated using the program DM (CCP4, 1994). This lack of density for a large region of sEGFR prevented complete refinement of this structure (Table 1).

Although we cannot discern precise details of the Fab11F8/sEGFR complex structure, several statements can be made from the partially refined structure (Figure 3A). First, it is clear that Fab11F8 interacts primarily (if not exclusively) with domain III, consistent with its ability to compete with both EGF and cetuximab for receptor binding. Second, it is clear that Fab11F8-bound sEGFR adopts the tethered configuration. Interpretable density could be seen for domain II starting from amino acid 239 which immediately precedes the dimerization arm. The dimerization arm makes all of the same contacts with domain IV that are observed in other structures of tethered sEGFR (Ferguson et al., 2003; Li et al., 2005). Indeed, the tethered conformation of sEGFR is strongly preferred in the absence of ligand (Dawson et al., 2007), and does not appear to be prevented by binding of Fab11F8 (or FabC225). Regarding our inability to define domain I in this structure, we note that domain I adopts two quite different positions with respect to domain III in previously published tethered sEGFR structures (Ferguson et al., 2003; Li et al., 2005). In comparing all four tethered sErbB structures published to date (two for sEGFR, and one each for sErbB3 and

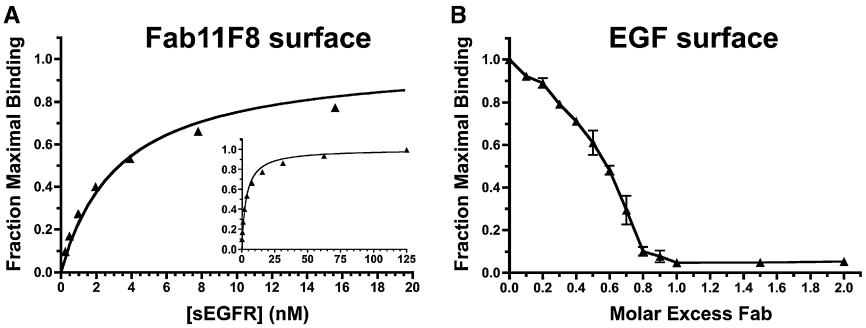

Figure 2. Fab11F8 Binds to sEGFR and Inhibits EGF Binding to sEGFR

(A) SPR analysis of sEGFR binding to immobilized Fab11F8. A series of sEGFR samples of the indicated concentrations was passed over a Biosensor surface to which Fab11F8 had been covalently coupled. A representative data set of the equilibrium SPR response for each sample, expressed as the fraction of the maximum binding, is plotted as a function of the concentration of sEGFR. The inset shows that no additional binding is seen at higher sEGFR concentrations. The curve indicates the fit to a simple one-site Langmuir binding equation for the data set shown. A K_D value of 3.3 ± 0.5 nM was obtained from at least three independent binding experiments.

(B) The ability of Fab11F8 to compete for sEGFR binding to immobilized EGF is shown. The indicated molar excesses of Fab were added to samples of fixed concentration of sEGFR (600 nM), and these samples were passed over immobilized EGF. The equilibrium SPR responses obtained for each sample, expressed as a fraction of the response with no added Fab, is plotted as a function of the molar excess of Fab. Error bars indicate the standard deviation of at least three independent measurements. All binding is abolished at a 1:1 stoichiometry of Fab11F8/sEGFR and the IC_{50} value for these conditions is 350 nM.

sErbB4), the most variable, and presumably most flexible, regions of domain II are immediately before and immediately after the dimerization arm. The relationship between domain I and the N-terminal part of domain II appear quite constant across these structures (Bouyain et al., 2005), as does the relationship between domain III and the C-terminal part of domain II (Dawson et al., 2007). By contrast, the relationship between the N- and C-terminal parts of domain II is more variable. In the absence of strong crystal packing contacts to hold domain I in a single orientation with respect to domain III in our Fab11F8/sEGFR complex, we suggest that domain I must adopt multiple orientations in the crystal, leading to our inability to place it in electron density maps.

Crystal Structure of Fab11F8 Bound to Isolated Domain III from sEGFR

Because the partially refined Fab11F8/sEGFR complex structure suggested that Fab11F8 binds exclusively to domain III (Figure 3A), we next analyzed 11F8 binding to isolated domain III from sEGFR (sEGFRd3). sEGFRd3 was produced in Sf9 cells infected with recombinant baculovirus that directs the expression of a protein comprising the native signal peptide of EGFR plus the first four amino acids of domain I fused to amino acids 311–514 of mature EGFR, followed by a hexahistidine tag (Li et al., 2005). Purification was as for sEGFR (Ferguson et al., 2000). Using SPR, we found that sEGFRd3 binds to immobilized Fab11F8 with a K_D value of 1.0 ± 0.1 nM (Figure 3B). Thus, Fab11F8 actually binds with slightly higher (~3-fold) affinity to sEGFRd3 than to full-length sEGFR, possibly because of some steric hindrance imposed by the other sEGFR domains. This contrasts starkly with the situation for EGF itself, which binds more weakly to sEGFRd3 than to full-length sEGFR (Kohda et al., 1993; Lemmon et al., 1997; Li et al., 2005). As depicted in Figure 1, both domains I and III of sEGFR are required to form the high-affinity sEGFR ligand binding site (Garrett et al., 2002; Ogiso et al., 2002).

In order to examine the details of Fab11F8 binding to sEGFRd3, we purified the Fab11F8/sEGFRd3 complex and grew crystals that diffracted to 2.6 Å resolution. The Fab11F8/sEGFRd3 complex structure was solved by MR methods using domain III of sEGFR and the Fv fragment of the Fab homology described above. The eight sEGFRd3 plus Fv fragments in the asymmetric unit of this crystal form were placed first using the program Phaser (McCoy, 2007). Subsequently the Fab constant regions (domains C_H1 and C_L) could be located. The model was manually rebuilt using electron density maps calculated with strict noncrystallographic symmetry constraints. Restraints were released in later stages of refinement (Table 1).

Fab11F8 binds to the more C-terminal end of domain III, and occludes 932 $Å^2$ of surface area on domain III from solvent (Figure 4; a total area of 1935 $Å^2$ is buried in the complex). All contacts between Fab11F8 and domain III come from the complementarity determining regions (CDRs) of the Fab, with approximately two thirds of the buried surface contributed by the V_H domain, and the remainder contributed by the V_L domain (Figure 3C). The shape complementarity parameter (Lawrence and Colman, 1993) for the Fab11F8/sEGFRd3 complex is 0.69, slightly higher than that typically observed (~0.65) for an antibody/antigen complex, consistent with the high affinity of Fab11F8 for its antigen. As shown in Figure 3D, interactions with domain III are contributed by CDRs 1 and 3 from the V_L domain (L1 and L3) plus CDRs 1, 2, and 3 from the V_H domain (H1, H2, and H3). CDR 2 from V_L (L2) makes no contacts. L1 and L3 from Fab11F8 contact the most C-terminal parts of the domain III epitope. The side chains of Q27 and Y32 (in L1) make close contacts or hydrogen bonds with the C-terminal strand of the domain III solenoid (or β helix) and the α helix that immediately follows it. L3 also makes main-chain-to-main-chain hydrogen bonds with this C-terminal region of domain III, with additional stabilization by one side-chain-to-main-chain hydrogen bond plus two water-mediated interactions (Figures 3D and 5A).

The majority of specific interactions between Fab11F8 and domain III involve the heavy-chain CDRs. H1 lies in the center of the V_H/domain III interface, and plays a role in coordinating interactions of H2 and H3. The two H1 side chains that make hydrogen bonds to domain III (D31B and Y33) interact with sEGFR residues that are also contacted by H2 side chains. Six of the ten side chains in H2 make hydrogen bonds with domain III (Figures 3D and 5A). Each H2 residue involved is a hydroxy amino acid (Y50, Y52, Y53, S56, and T57) or an acidic residue (D58), as is typical for CDR-mediated interactions of high-affinity antibodies isolated from phage-display screens (Fellouse et al., 2005). H3 presents two hydrophobic side chains (I97 and F98) that occupy

Table 1. Data Collection and Refinement Statistics

	Fab11F8/sEGFRd3 Complex	Fab11F8/sEGFR Complex
Data Collection[a]		
Space group	$P2_1$	$C222_1$
Unique cell dimensions	a = 154.4 Å, b = 139.1 Å, c = 175.3 Å; β = 90.02°[b]	a = 77.8 Å, b = 70.9 Å, c = 147.1 Å
X-ray source	CHESS F2	CHESS A1
Resolution limit	2.6 Å	3.3 Å
Observed/unique	875,685/231,396	132,555/21,995
Redundancy	3.8-fold	6-fold
Completeness (%)	95.6 (96.8)	100.0 (100.0)
R_{sym}[c]	0.097 (0.456)	0.188 (0.580)
$\langle I/\sigma \rangle$	13.1 (2.4)	9.13 (3.1)
Refinement		
Resolution limits (Å)	43–2.6	130–3.3
Number of reflections/number in test set	231,396/11,664	21,865/1,120
R factor (R_{free})[d]	0.23 (0.29)	0.28 (0.37)
Model		
Protein	8 Fab11F8/sEGFRd3 complexes	1 Fab11F8/sEGFR complex
	Residues 310–502 (sEGFRd3)[e]	Residues 239–613 (sEGFR)
	Residues 1–213 (light chain)	Residues 1–213 (light chain)
	Residues 1–222 (heavy chain); missing residues 137–141[f]	Residues 2–222 (heavy chain)
	64 saccharide units	9 saccharide units
	1,035 water molecules, 8 sulfate ions	
Total number of atoms	39,037	5,645
Rmsd bond lengths (Å)	0.012	0.022
Rmsd bond angles (°)	1.44	2.64

[a] Numbers in parentheses refer to last resolution shell.
[b] Despite the small deviation of β from 90°, these data could not be merged in an orthorhombic point group.
[c] $R_{sym} = \Sigma|I_h - \langle I_h \rangle|/\Sigma I_h$, where $\langle I_h \rangle$ = average intensity over symmetry-equivalent measurements.
[d] R factor = $\Sigma|F_o - F_c|/\Sigma F_o$, where summation is over data used in the refinement; R_{free} includes only 5% of the data excluded from the refinement.
[e] Chains A and M start at 308; chains B, E, and S start at 309.
[f] Number of missing amino acids varies by chain, with a maximum of eight amino acids missing (chain C).

a hydrophobic pocket on the surface of domain III (Figures 3D and 5A). This is the same pocket that accommodates the essential leucine side chain of the EGFR-activating ligands (L47 in EGF and L48 in TGFα), providing one clear explanation for why Fab11F8 binding and EGF binding to sEGFR are mutually exclusive. The H3 hydrophobic loop is held in place in part by the H1 loop, which makes hydrogen bonds with sEGFR residues H409, S418, and S440 at the periphery of this critical hydrophobic pocket.

Fab11F8 Recognizes the Same sEGFR Epitope as FabC225

The epitope for Fab11F8 on domain III overlaps almost exactly with that recognized by cetuximab (Li et al., 2005). The 932 $Å^2$ Fab11F8 epitope (red in Figure 4A) corresponds remarkably closely to the 882 $Å^2$ FabC225 epitope (yellow in Figure 4A) in both extent and location. Despite this correspondence, the details of the interactions made by Fab11F8 are quite different from those seen with cetuximab (see below). Although competition with cetuximab was a component of the procedure used to select Fab11F8, the almost precise correspondence of the epitopes is remarkable and suggests that this surface possesses features that make it particularly well suited for antibody recognition. Approximately 60% of the Fab11F8 epitope is also included in the EGF binding site on domain III (blue in Figure 4A).

We asked what features of this surface of sEGFRd3 might account for this coincidence of binding sites, and summarize some observations in Figure 4. The surface of domain III that binds EGF, Fab11F8, and cetuximab is relatively flat, with the exception of the hydrophobic pocket that accommodates a critical EGF/TGFα leucine or key aromatic groups from the antibodies. The central hydrophobic region is encircled by positively charged and other hydrophilic amino acids (Figure 4B), reminiscent of the organization seen in other protein/protein interaction sites (Clackson et al., 1998). The epitopes also coincide with a region of positive electrostatic potential on sEGFRd3 (Figure 4B) that complements negative potential in the Fab paratopes.

Another feature of the sEGFR surface that should be considered in identifying likely binding sites for therapeutic antibodies is the degree of glycosylation. The extracellular region of sEGFR

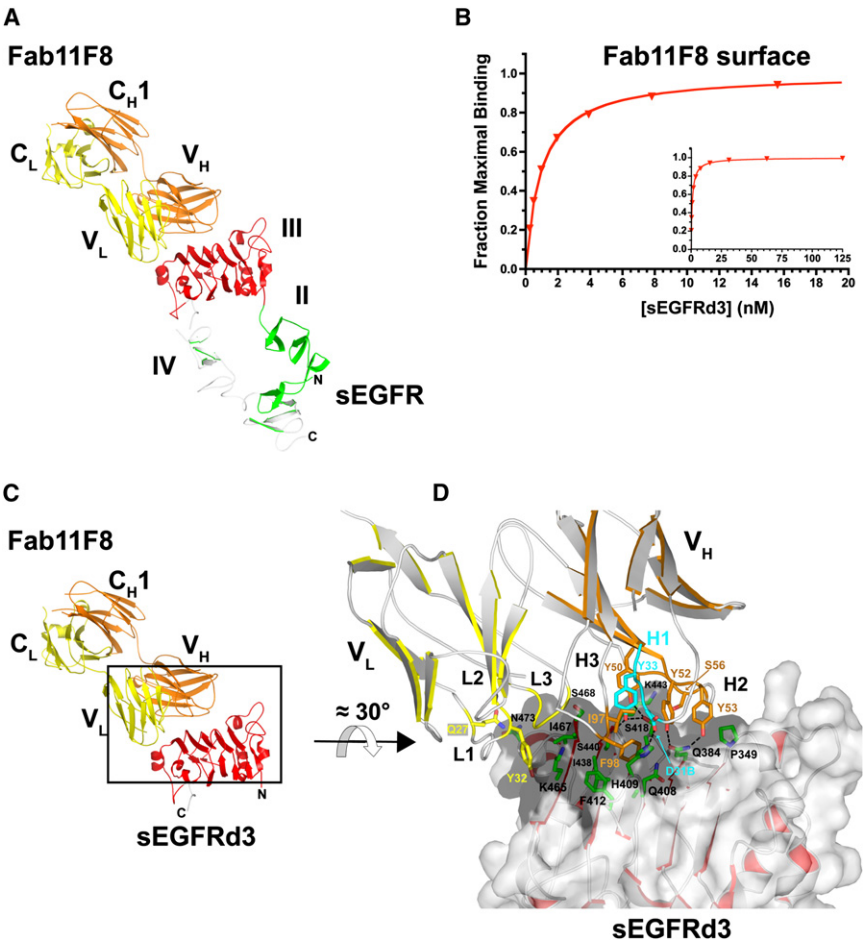

Figure 3. Fab11F8 Binds to Domain III of sEGFR

(A) Cartoon of the Fab11F8/sEGFR complex. The light chain of Fab11F8 is shown in yellow, and the heavy chain in orange. Domains of sEGFR are colored as in Figure 1.

(B) SPR analysis of sEGFRd3 binding to immobilized Fab11F8 performed and analyzed as described in Figure 2A. A K_D value of 1.0 ± 0.1 nM was obtained.

(C) Cartoon of the Fab11F8/sEGFRd3 complex in the same orientation and colors as in (A).

(D) Detailed view of the Fab11F8/sEGFRd3 interface, rotated ≈30° about a horizontal axis with respect to (C). Secondary structure is highlighted in yellow for V_L and orange for V_H. The parts of the CDRs that interact with domain III are yellow for L1 and L3, cyan for H1, and orange for H2 and H3. Side chains that make direct hydrogen bond or key van der Waals contacts are shown in stick representation in colors as for the interacting CDRs. The main chain of domain III of sEGFR is show in a gray cartoon highlighted in red. Side chains on domain III that make key contacts with the Fab are shown in green stick representation and labeled in black. A transparent molecular surface is show around domain III. The darker gray shading indicates the region of this surface that is occluded from solvent by the interaction with Fab11F8, defined using the program CNS (Brunger et al., 1998).

is ~20% carbohydrate by mass, with ten glycosylation sites (Zhen et al., 2003), four on domain III. In Figures 4C and 4D, high-mannose oligosaccharide chains have been placed at each glycosylation site on the receptor, guided by the one or two saccharide units observed in the crystal structures. Because the oligosaccharides will be highly mobile, this model is intended only to give a sense of scale of the surface glycosylations on EGFR. As a result of their mobility, the carbohydrates would likely occlude (at least partially) much larger areas of the surface than suggested here. Two faces of the domain III solenoid are highly occluded by carbohydrate, and are therefore less likely to be significant sites of antibody interaction. In addition, a sugar chain on domain IV will impact part of the domain III surface. The region of the domain III surface that includes the Fab11F8 and FabC225 epitopes plus the EGF/TGFα binding site corresponds to the area on the surface that is the most unfettered by oligosaccharides (Figure 4C). This issue is likely to provide a large part of the explanation as to why the epitopes for Fab11F8 and cetuximab are so very similar. It would be difficult to select an overlapping epitope of similar surface area that is not influenced by nearby oligosaccharides to at least some degree. There are few other regions on the surface of sEGFR that share these characteristics (as shown in Figure 4D for electrostatic potential and carbohydrate occlusion). A combination of electrostatic and carbohydrate steering likely promotes association of binding partners with the flat, hydrophobic face of domain III.

The Same sEGFR Epitope Is Recognized by Quite Distinct Sets of Fab Interactions

Although Fab11F8 and FabC225 share essentially the same epitope on sEGFRd3, they recognize it with sets of interactions that are clearly different (Figure 5). L1 is the only antigen-binding loop that shows significant sequence similarity between the two Fabs (Figure 5C), and the side chain of Q27 in L1 interacts with N473 on domain III in both complexes (Figures 5A and 5B). L2, which does not form part of the Fab11F8 paratope (Figure 5A), contributes an important tyrosine side chain (Y50) in the FabC225/sEGFRd3 interface (Figure 5B) that takes the place of Y32 in L1 of Fab11F8. L3 plays a broadly similar role in Fab11F8 and FabC225 interaction with sEGFRd3, making primarily backbone-mediated interactions with the C-terminal strand of the domain III solenoid (Figures 5A and 5B).

Interactions mediated by the V_H CDRs show less commonality between the two Fabs. H1 is involved in Fab11F8 but not FabC225 binding to sEGFRd3. H2 from Fab11F8 and FabC225 interact with essentially the same set of residues in sEGFRd3, but employ an entirely different set of residues and interaction types to do so. Despite their sequence differences, H3 from the two Fabs both project hydrophobic side chains into the previously mentioned apolar pocket that EGF binding also employs. Fab11F8 projects the I97 and F98 side chains into this pocket, whereas FabC225 projects Y98. Beyond this, it is notable that H3 is highly enriched in hydroxy amino acids (TYYDY) in

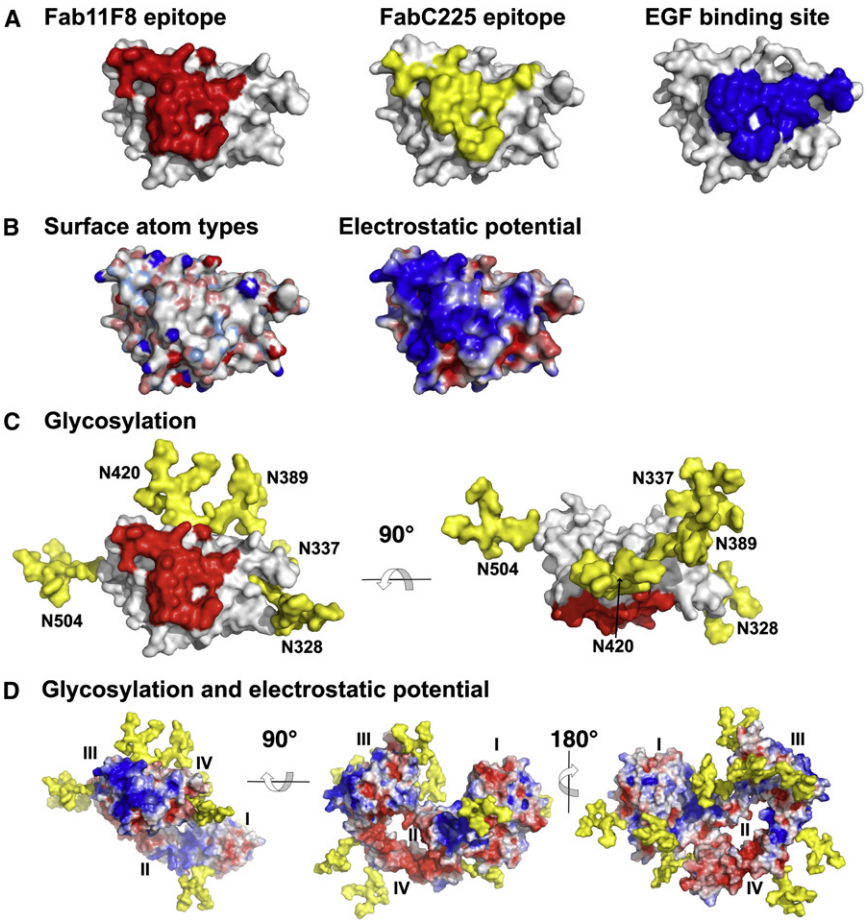

Figure 4. Features of the Shared Fab11F8, FabC225, and EGF Binding Region on Domain III

(A) Molecular surface representations of domain III of sEGFR with the contact regions (as defined in Figure 3D) colored red for Fab11F8, yellow for FabC225, and blue for EGF. Orientation is looking down onto the domain III binding site.

(B) Functional features of the domain III molecular surface. In the left panel, the surface is colored by atom type: negative, red; positive, blue; polar oxygen, pink; polar nitrogen, light blue; and apolar, white. The right panel shows the electrostatic potential from −2.5 kT (red) to +2.5 kT (blue) projected onto the surface. Electrostatic potential calculations used the adaptive Poisson-Boltzmann solver (APBS) implemented in PyMOL (Baker et al., 2001; DeLano, 2004).

(C) Orthogonal views of domain III. High-mannose chains (yellow) have been placed at each position of glycosylation on sEGFR guided by the one or two ordered sugar groups that are seen in the X-ray crystal structures. For reference, the contact region of Fab11F8 is shown (red).

(D) Three orientations of sEGFR are shown with the electrostatic potential, as in (B), projected on the surface and high-mannose chains shown. Both electrostatic and carbohydrate steering might play a role in guiding Fabs or ligands to the shared binding site on domain III.

FabC225, whereas H2 has this characteristic in Fab11F8. This allows the FabC225 H3 to participate in hydrogen bonding that requires involvement of H1 in the Fab11F8 case.

The distinct sets of sEGFR interactions made by Fab11F8 and FabC225 suggest a difference in their pH sensitivity. It is well known that growth factor binding to EGFR is highly pH sensitive, and that pH sensitivity affects ligand/receptor trafficking (French et al., 1995; Nunez et al., 1993). TGFα binding is highly pH sensitive and the ligand/receptor complex will dissociate very early in the endocytic pathway, leading to receptor recycling. EGF binding is less sensitive to pH, and EGF-stimulated EGFR is trafficked to lysosomes for degradation (Waterman et al., 1998). Protonation (at low pH) of central histidines observed in the ligand/receptor binding interface are thought to disrupt the interaction (Garrett et al., 2002; Ogiso et al., 2002). There is likely no such low-pH disruption of Fab11F8 or FabC225 complexes with EGFR. H409 in sEGFRd3 forms a hydrogen bond with a D31B in Fab11F8 (Figure 5A). Protonation of this histidine would actually be expected to increase (rather than decrease) the strength of Fab11F8 binding. We were able to detect a modest (~2-fold) increase in the affinity of sEGFR for immobilized Fab11F8 at pH 5.0 relative to that observed at pH 8.0 (data not shown). FabC225/sEGFR interaction is likely to be insensitive to pH, because the interface contains no groups expected to titrate at physiological pH values (Li et al., 2005). The fact that the affinity of these antibodies for EGFR is not reduced at low pH is likely important for the component of their therapeutic action that involves the promotion of EGFR downregulation by internalization and lysosomal trafficking (Sunada et al., 1986).

Effects of Mutations in the sEGFRd3 Epitope

To gain insight into how binding energy is apportioned across the Fab11F8/sEGFR interface, we generated mutations at six positions in sEGFR (ringed in Figures 5A and 5B), and analyzed the effects on binding to Fab11F8, FabC225, and EGF (Figure 6). An alanine substitution at N473, which interacts with Q27 in L1 of Fab11F8 and FabC225, actually increased Fab affinity by ~1.5-fold, but reduced binding to EGF (which it does not actually contact) by approximately the same amount. We speculate that these small affinity changes reflect a loss of structural restraints involving the N473 side chain that promote an optimal EGF-binding configuration but oppose the conformation that is most favorable for Fab binding. The side chain of S468 forms a hydrogen bond with the Fab11F8 main chain, and lies adjacent to a hydrophobic pocket that accommodates the Y33 and Y50 side chains of the Fab (Figure 5A). In the FabC225 complex, S468 forms a hydrogen bond with the Y100A side chain. We reasoned that placing a large aliphatic side chain at this position could improve packing interactions in the hydrophobic pocket, although hydrogen bonds would be lost with L3 or H3. An S468I mutation increased the affinity of Fab11F8 for sEGFR by almost 4-fold. A more modest affinity increase (~1.4-fold) was seen for

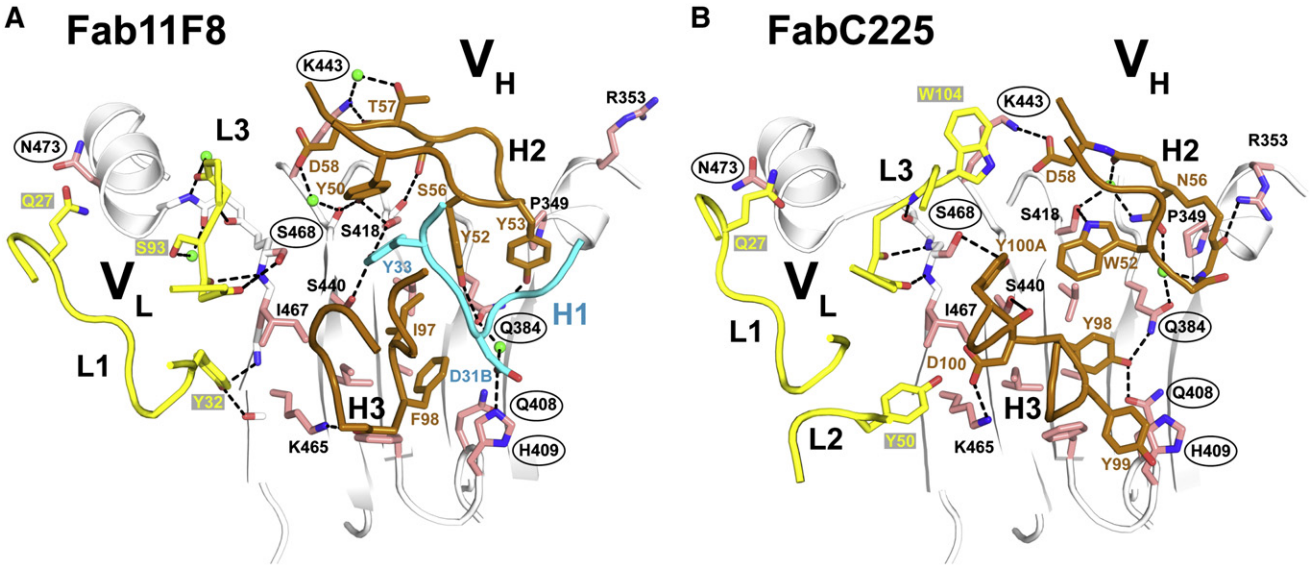

C

```
Chothia #                .          .          .          .          .          .          .
Fab11F8 V_L   EIVMTQSPAT LSLSPGERAT LSCRASQSVS SYLAWYQQKP GQAPRLLIYD ASNRATGIPA RFSGSGSGTD
FabC225 V_L   D.LL....VI ..V.....VS F.....IG TNIH....RT NGS.....KY ..ESIS...S ..........
CDRs                                    L1                     L2
Chothia #                .          .          .
Fab11F8 V_L   FTLTISSLEP EDFAVYYCHQ YGSTPLTFGG GTKAEIK
FabC225 V_L   ...S.N.V.S ..I.D...Q. NNNW.T..A ...L.L.
CDRs                               L3

Chothia #                .          .          .  AB       .          .          .
Fab11F8 V_H   QVQLQESGPG LVKPSQTLSL TCTVSGGSIS SGDYYWSWIR QPPGKGLEWI GYIYYSGSTD YNPSLKSRVT
FabC225 V_H   ....KQ.... ..Q..QS..I ......F.LT N--YGVH.V. .S.......L .V.WSG.N.. ..TPFT..LS
CDRs                                    H1                     H2
Chothia #     .          .  ABC        .          .ABC       .
Fab11F8 V_H   MSVDTSKNQF SLKVNSVTAA DTAVYYCARV SIFGVGTFDY WGQGTLVTVS S
FabC225 V_H   INKDN..S.V FF.M..LQSN ...I.....A LTYYDYE.A. .......... A
CDRs                                    H3
```

Figure 5. Fab11F8 and FabC225 Use Distinct Interactions to Recognize a Common Epitope

(A and B) Detailed view of the interactions of domain III of sEGFR with Fab11F8 (A) and FabC225 (B). The orientation is as in Figure 4A. Only those parts of Fabs that are involved in binding are shown. Interacting CDRs are colored as in Figure 3D. Side chains from the Fab that interact with sEGFR are shown in stick representation and labeled using the same color scheme. The epitope region on sEGFR is shown in white cartoon. Side chains from sEGFRd3 that interact with the Fab are shown in stick representation in pink with black labels. The same set of side chains on the sEGFR are shown in both panels. For clarity, side chains that line the hydrophobic binding pocket on domain III (F412, A415, V417, and I438) are not labeled. Hydrogen bonds are shown with dotted black lines. Key water molecules are shown as green spheres. Side chains on sEGFRd3 that are altered in analysis of the binding site mutations (Figure 6) are ringed.

(C) Amino acid sequence alignment of the variable domains of Fab11F8 and FabC225. Only nonidentical amino acids are shown for FabC225, with a period indicating identity with Fab11F8 and a dash indicating a gap. Amino acids involved in interacting with domain III are highlighted using the same colors as in (A). A dot above every tenth amino acid indicates Chothia numbering that is used in the text and all figures (Chothia et al., 1986). Chothia-defined CDRs are underlined and Kabat-defined CDRs are indicated by bold text. In the submitted PDB files, and in Li et al. (2005), the Fab amino acids are numbered sequentially.

FabC225, and EGF binding was slightly reduced. Interestingly, combining the effects of mutating N473 and S468 resulted in a loss in FabC225 binding affinity, but maintained an approximate 2-fold increase in Fab11F8 affinity. These findings suggest that van der Waals complementarity of the Fab11F8/sEGFR interface is suboptimal. In turn, this observation suggests that alterations in Fab11F8 itself could be made that would improve van der Waals packing across the interface, and allow higher-affinity binding. With this in mind, the structure presented here provides a framework for designing mutations in Fab11F8 that will bind to EGFR with even higher affinity, using structure-based computational methods of the sort recently described for the affinity enhancement of an already high affinity antibody against an integrin I domain (Clark et al., 2006). Such an affinity matured

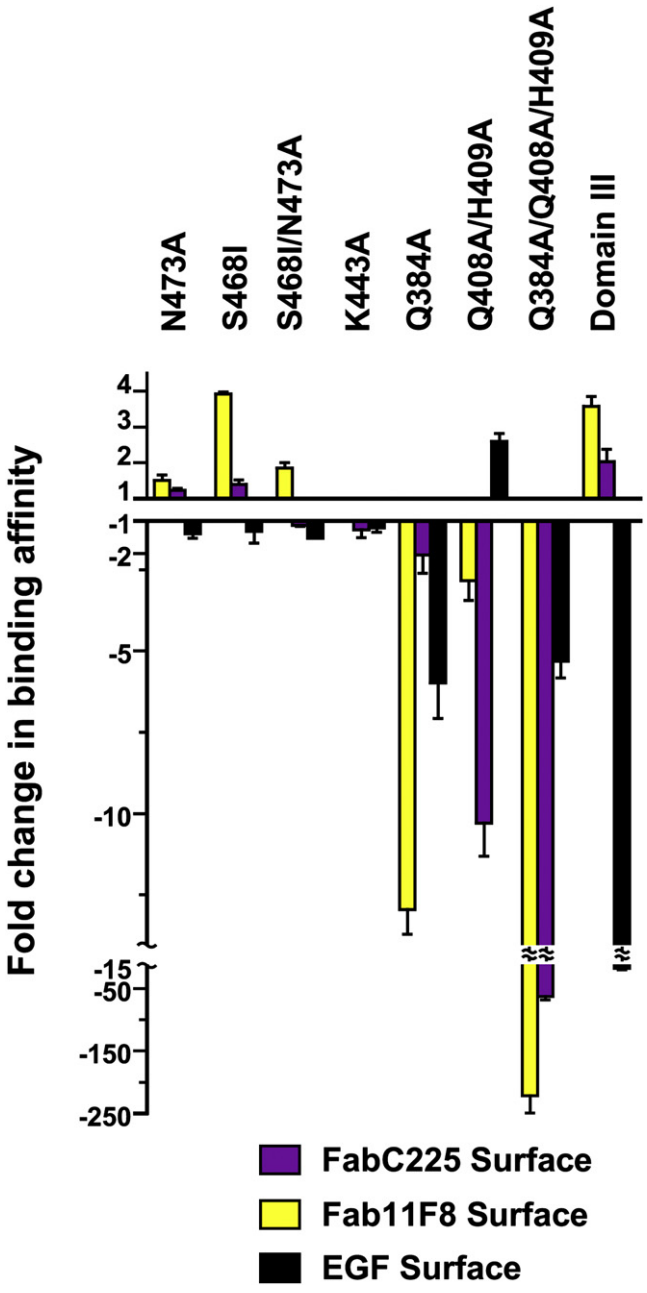

Figure 6. Effect of Alterations in Domain III on the Affinity of sEGFR for Fab11F8, FabC225, and EGF

The fold change relative to wild-type sEGFR of the binding affinity for each indicated altered sEGFR to immobilized Fab11F8 (yellow), FabC225 (magenta), and EGF (black). K_D values of wild-type sEGFR, determined as described in Figure 2, are 3.3 ± 0.5 nM (Fab11F8), 2.3 ± 0.5 nM (FabC225), and 130 ± 4 nM (EGF). Positive (upward) fold changes indicate higher-affinity binding, while negative (downward) fold changes indicate weaker binding. Error bars indicate the standard deviation for at least three separate measurements.

version of IMC-11F8 might prove to be an even better therapeutic agent. It is also been suggested that very high-affinity targeted antibodies might actually have less therapeutic value, owing to a restriction in tumor penetration (Adams et al., 2001). The structure presented here would also provide a framework to design lower-affinity variants of IMC-11F8.

Other mutations in the Fab11F8/sEGFR interface had the anticipated effects. Mutation of K443 to alanine had no effect on Fab11F8 and only slightly reduced the affinity of sEGFR for FabC225 and EGF. Similarly, mutation of Q384, Q408, or H409 to alanine, alone or in combination, reduced the affinity of sEGFR for Fabs and EGF. Mutating any of these residues will remove important hydrogen-bonding interactions and van der Waals contacts (Figures 5A and 5B). One exception was the Q408A/H409A mutation that actually increased EGF binding by ~2.5-fold, probably because Q408 abuts hydrophobic residues of EGF in the sEGFR/EGF complex.

Glycosylation and Crystal Packing Contacts

One notable feature of the packing of the domain III molecules in the Fab11F8/sEGFRd3 crystal is the role of carbohydrate. It is typically considered that carbohydrates are too flexible to form crystal packing interactions and the prevailing view is that deglycosylation of a glycoprotein should be a prerequisite for crystallographic studies (Baker et al., 1994). In the Fab11F8/sEGFRd3 crystal, there are multiple examples of sugar moieties contributing to packing interactions. For example, over a third of a 974 $Å^2$ interface between one pair of Fab11F8/sEGFRd3 complexes in the asymmetric unit is contributed by domain III oligosaccharides. Where these oligosaccharides contribute to crystal packing, three or more well-ordered sugar residues were observed, whereas at equivalent positions on other domain III molecules, only a single or at most two ordered saccharide units are seen. Interestingly, oligosaccharides also contributed to packing interactions in the FabC225/sEGFR complex (Li et al., 2005). For one crystal packing contact in the FabC225 complex, more than 60% of the 600 $Å^2$ interface area involves sugar groups. Deglycosylation would have hampered formation of these crystal forms. Instability of deglycosylated sEGFR and sEGFRd3 precluded attempts to obtain crystals of the deglycosylated proteins.

Comparison of the Structures of the Bound Fab Fragments of IMC-11F8 and Cetuximab

A critical difference between IMC-11F8 and cetuximab that is important for the use of these antibodies as anticancer drugs is that the variable domains of IMC-11F8 are of human origin, whereas the variable region of cetuximab is of mouse origin. Given their distinct sequence origin, it is worthwhile to compare the overall structures of the Fab fragments from IMC-11F8 and cetuximab. They are very similar. The elbow angle for the Fab11F8 in the complex is 173° ± 1° (among the eight copies in the asymmetric unit), which is within the normal range (Stanfield et al., 2006). This is larger than for FabC225 when bound to sEGFR (150°) and significantly greater than for uncomplexed FabC225 (135°).

The V_L domains of each Fab are remarkably similar. The root-mean-square deviation (rmsd) upon superimposing all main-chain atoms in the V_L domain is 0.77 Å. This similarity extends to the CDRs that deviate no more between the two structures than other loops in this domain (Figure 7A). This is not unexpected, because the V_L CDRs of each antibody belong to the same Chothia canonical classes (class 2, 1, and 1 for L1, L2, and L3) (Al-Lazikani et al., 1997). The majority of the interactions

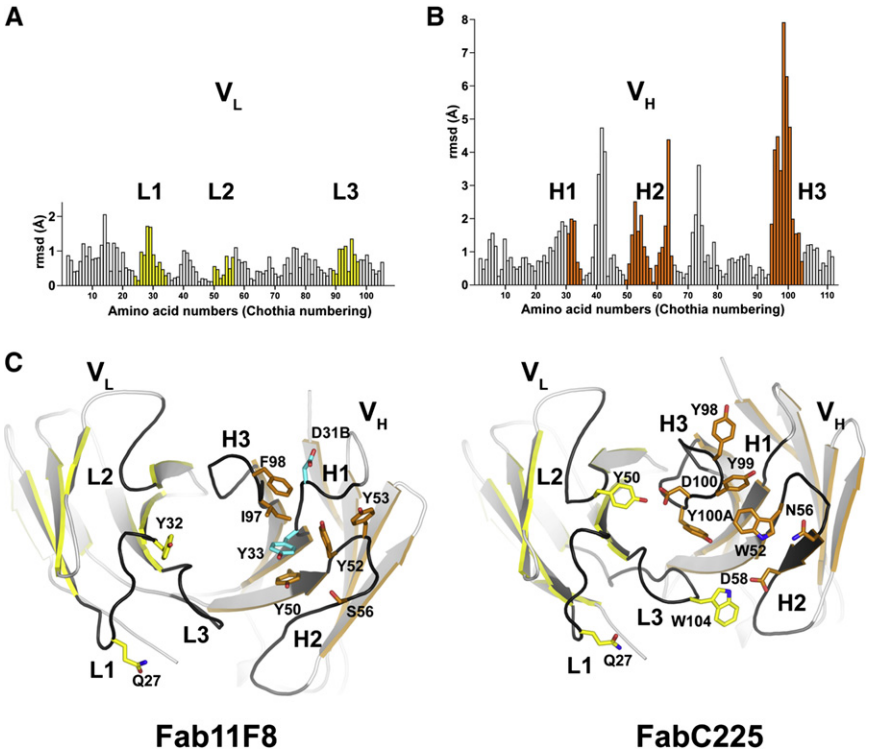

Figure 7. Comparison of the Structures of Fab11F8 and FabC225

(A and B) The root-mean-square deviation (rmsd) of Cα positions between Fab11F8 and FabC225 for V_L domains (A) and V_H domains (B). Backbone atoms for each pair of domains were individually superimposed using the program SUPERPOSE (CCP4, 1994). The CDRs are marked and highlighted in yellow for V_L and orange for V_H.

(C) Cartoons of the variable domains of Fab11F8 and FabC225 looking up from the domain III binding site. Kabat CDRs are in dark gray. Key side chains in the paratope are shown in stick representation and colored as in Figure 3D.

between sEGFR and the light chains of Fab11F8 and FabC225 are backbone hydrogen bonds (Figures 5A and 5B), particularly in the case of L3. The conservation of the light-chain CDR structures between the two Fabs is likely to be important in defining their similarly high affinities for EGFR.

When comparing Fab11F8 and FabC225 V_H domains (Figure 7B), it is clear that there are much larger main-chain deviations. The rmsd is 1.78 Å for all main-chain atoms in the V_H domain (excluding the insertion in H1 of Fab11F8) and there are substantial (>2 Å) deviations in the main-chain positions for each CDR, with the greatest differences in H3 (Figure 7B). These loops serve as scaffolds to present the side chains that interact with domain III of EGFR (Figure 7C) and, as explained above, the V_H interactions with sEGFR are quite different for the two antibodies, although they recognize almost identical epitopes.

Implications for IMC-11F8 as an EGFR-Targeted Therapeutic

In addition to binding very similar epitopes, Fab11F8 and FabC225 (Li et al., 2005) adopt almost identical orientations

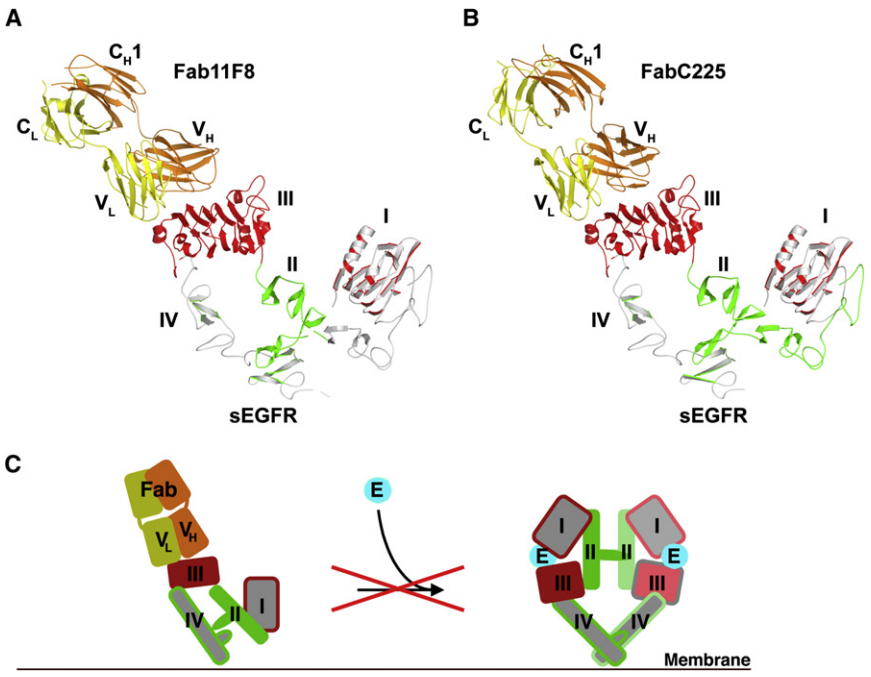

Figure 8. Mechanism of Inhibition of EGFR Activation by IMC-11F8 and by Cetuximab

(A) Cartoon model of Fab11F8 bound to sEGFR colored as in Figure 3A. Domain I and the N-terminal portion of domain II (gray) have been modeled using the coordinates from PDB ID code 1YY9.

(B) Cartoon of the FabC225/sEGFR complex (PDB ID code: 1YY9) colored as in (A).

(C) The mechanism of inhibition of ligand-induced dimerization and activation of EGFR for IMC-11F8 and cetuximab based on the structures presented here and in Li et al. (2005). The binding of the antibody to domain III of EGFR prevents ligand binding and might also sterically inhibit the conformational change that must occur for dimerization.

when bound to sEGFR. Figure 8A compares the structure of Fab11F8 bound to full-length sEGFR (modeled based on the Fab11F8/sEGFRd3 complex) with the FabC225/sEGFR complex. One of the key features that defines the orientation of both Fabs with respect to the domain III surface (and thus with respect to sEGFR) is the close approach of L3 to the C-terminal region of the domain III solenoid, together with a similarly organized array of L1 interactions (Figures 5A and 5B). With an almost identical epitope, a very similar binding orientation, and a very similar binding affinity, IMC-11F8 is likely to exert its effects on EGFR inhibition through precisely the same mechanisms as cetuximab, which we have discussed previously (Li et al., 2005). Both antibody drugs block the ligand binding site on domain III of EGFR, and (because of their high affinity for EGFR) can prevent EGF from activating the receptor (Figure 8B). In addition, the mode of EGFR binding exhibited by both IMC-11F8 and cetuximab is such that both antibodies will sterically prevent the extracellular region of the receptor from adopting the extended conformation that is required for dimerization. Thus, screening of a human Fab library for an antibody that can bind and inhibit EGFR and competes with cetuximab for receptor binding has yielded an antibody that is remarkably similar to cetuximab in its properties—although quite different in the details of its antigen combining site. It seems unlikely that such a screen would isolate an antibody so similar to cetuximab unless there is something unique about the epitope that both recognize, including the properties that we have discussed above. Alternatively, the mode of EGFR binding observed for IMC-11F8 and cetuximab might be uniquely suited to EGFR inhibition. In either case, the approach has yielded a fully human antibody that has very similar properties to the chimeric cetuximab. Cetuximab has already shown its value in the clinic but suffers from the problems associated with immune sensitivity to mouse-derived antibody sequences. IMC-11F8 as a mechanistically very similar, but fully human, antibody is likely to reproduce all of cetuximab's promise, but lack its disadvantages.

EXPERIMENTAL PROCEDURES

Crystallization and Data Collection

sEGFR and sEGFRd3 were produced as described (Ferguson et al., 2000; Li et al., 2005). The Fab fragment of IMC-11F8 (Fab11F8) was prepared by papain cleavage of the IgG protein. Fab11F8 complexes with sEGFR and sEGFRd3 were purified as described (Li et al., 2005) and crystallized by the hanging drop vapor diffusion method. Drops containing equal parts of Fab11F8/sEGFR (10 mg/ml) and of reservoir (12% PEG3350, 1 M NaCl, 50 mM MES [pH 6.5]) were equilibrated over this reservoir at 25°C. To limit nucleation and promote growth of large single crystals, the crystallization trays were sequentially moved to conditions of decreasing temperature over 2 weeks, ending at 4°C. Equal parts Fab11F8/sEGFRd3 (6 mg/ml) complex and reservoir (12% PEG3350, 250 mM $[NH_4]_2SO_4$, 50 mM sodium acetate [pH 5.0]) were equilibrating over this reservoir at 25°C. Streak seeding produced large single crystals. In each case, crystals were briefly exposed to a cryostabilizer of reservoir supplemented with 15% ethylene glycol and flash-frozen in liquid nitrogen. X-ray diffraction data (Table 1) were collected at the Cornell High Energy Synchrotron Source (CHESS). Data were processed using HKL2000 (Otwinowski and Minor, 1997).

Structure Determination and Refinement

MR methods were used to solve both structures. Search models for sEGFR were from PDB ID code 1YY9. For Fab11F8, a homology model was generated using the program MODELLER (Eswar et al., 2006) using the light chain from PDB ID code 1DN0 and heavy chain from PDB ID code 1CE1. For Fab/sEGFR, an initial solution was found for the Fab plus domain III of sEGFR using the program MOLREP (Vagin and Teplyakov, 1997). Attempts to locate domains I, II, and IV using MR methods were unsuccessful. Following rounds of manual model building in O (Jones et al., 1991) and refinement combined with density modification using the programs REFMAC and DM (CCP4, 1994), interpretable density was seen for domain IV and part of domain II of sEGFR. No interpretable density could be seen for domain I. The current model packs to form disconnected layers. At least some of domain I must be present, but this region of sEGFR is presumably statically disordered.

For Fab11F8/sEGFRd3, an initial MR search employed two model fragments: domain III of sEGFR and the Fv region of the Fab homology model. Eight copies of each fragment were located using automatic search protocols in the program Phaser (McCoy, 2007). With the positions of these eight Fv/sEGFRd3 fragments fixed, the eight Fab constant regions (domains C_H1 and C_L) could be located. The noncrystallographic symmetry (NCS) relationship between the eight Fv/sEGFRd3 fragments and the C_H1/C_L fragments differs slightly. Eight-fold NCS averaging was applied to generate an electronic density map using the program DM (CCP4, 1994) and the model was rebuilt using the program Coot (Emsley and Cowtan, 2004). Later stages of refinement, using the program REFMAC (CCP4, 1994), used no NCS restraints.

Generation of Binding Site sEGFR Mutations

Standard PCR directed mutagenesis was used to produce the appropriate DNA in the pFastBac vector. The following mutations were made: Q408A/Q409A, Q384A/Q408A/Q409A, K443A, S468I, N473A, and S468I/N473A. Altered sEGFRs were produced exactly as for wild-type sEGFR (Ferguson et al., 2000).

Binding Studies

Fab11F8 (50 μg/ml in 10 mM sodium acetate [pH 5.5]) was amine coupled to a CM5 BIAcore sensor chip and SPR was used to measure binding of wild-type and mutated versions of sEGFR to immobilized Fab11F8 as described (Li et al., 2005). The effect of added Fab11F8 upon the binding of 600 nM sEGFR to immobilized EGF was determined as described (Li et al., 2005).

ACKNOWLEDGMENTS

We thank Mark Lemmon and members of the Ferguson laboratory for valuable discussions and critical comments and Nicole Covino (ImClone Systems) for valuable technical assistance. K.M.F. is supported by a Career Award in the Biomedical Sciences from the Burroughs Wellcome Fund, and by NCI grant R01-CA112552. K.M.F. is the Dennis and Marsha Dammerman Scholar supported by the Damon Runyon Cancer Research Foundation (DRS-52-06). This work is based upon research conducted at CHESS, which is supported by the NSF under award DMR 97-13424, using the Macromolecular Diffraction at CHESS (MacCHESS) facility, which is supported by award RR-01646 from the NIH, through its National Center for Research Resources. P.K. is an employee of ImClone Systems, the developer of IMC-11F8. This work was supported in part by a grant from ImClone Systems.

Received: August 31, 2007
Revised: November 18, 2007
Accepted: November 19, 2007
Published: February 12, 2008

REFERENCES

Adams, G.P., Schier, R., McCall, A.M., Simmons, H.H., Horak, E.M., Alpaugh, R.K., Marks, J.D., and Weiner, L.M. (2001). High affinity restricts the localization and tumor penetration of single-chain Fv antibody molecules. Cancer Res. *61*, 4750–4755.

Al-Lazikani, B., Lesk, A.M., and Chothia, C. (1997). Standard conformations for the canonical structures of immunoglobulins. J. Mol. Biol. *273*, 927–948.

Baker, H.M., Day, C.L., Norris, G.E., and Baker, E.N. (1994). Enzymatic deglycosylation as a tool for crystallization of mammalian binding proteins. Acta Crystallogr. D Biol. Crystallogr. *50*, 380–384.

Baker, N.A., Sept, D., Joseph, S., Holst, M.J., and McCammon, J.A. (2001). Electrostatics of nanosystems: application to microtubules and the ribosome. Proc. Natl. Acad. Sci. USA *98*, 10037–10041.

Bouyain, S., Longo, P.A., Li, S., Ferguson, K.M., and Leahy, D.J. (2005). The extracellular region of ErbB4 adopts a tethered conformation in the absence of ligand. Proc. Natl. Acad. Sci. USA *102*, 15024–15029.

Brunger, A.T., Adams, P.D., Clore, G.M., DeLano, W.L., Gros, P., Grosse-Kunstleve, R.W., Jiang, J.S., Kuszewski, J., Nilges, M., Pannu, N.S., et al. (1998). Crystallography & NMR system: a new software suite for macromolecular structure determination. Acta Crystallogr. D Biol. Crystallogr. *54*, 905–921.

Burgess, A.W., Cho, H.S., Eigenbrot, C., Ferguson, K.M., Garrett, T.P., Leahy, D.J., Lemmon, M.A., Sliwkowski, M.X., Ward, C.W., and Yokoyama, S. (2003). An open-and-shut case? Recent insights into the activation of EGF/ErbB receptors. Mol. Cell *12*, 541–552.

CCP4 (Collaborative Computational Project, Number 4) (1994). The CCP4 suite: programs for protein crystallography. Acta Crystallogr. D Biol. Crystallogr. *50*, 760–763.

Cho, H.S., and Leahy, D.J. (2002). Structure of the extracellular region of HER3 reveals an interdomain tether. Science *297*, 1330–1333.

Cho, H.S., Mason, K., Ramyar, K.X., Stanley, A.M., Gabelli, S.B., Denney, D.W., Jr., and Leahy, D.J. (2003). Structure of the extracellular region of HER2 alone and in complex with the Herceptin Fab. Nature *421*, 756–760.

Chothia, C., Lesk, A.M., Levitt, M., Amit, A.G., Mariuzza, R.A., Phillips, S.E., and Poljak, R.J. (1986). The predicted structure of immunoglobulin D1.3 and its comparison with the crystal structure. Science *233*, 755–758.

Clackson, T., Ultsch, M.H., Wells, J.A., and de Vos, A.M. (1998). Structural and functional analysis of the 1:1 growth hormone:receptor complex reveals the molecular basis for receptor affinity. J. Mol. Biol. *277*, 1111–1128.

Clark, L.A., Boriack-Sjodin, P.A., Eldredge, J., Fitch, C., Friedman, B., Hanf, K.J., Jarpe, M., Liparoto, S.F., Li, Y., Lugovskoy, A., et al. (2006). Affinity enhancement of an in vivo matured therapeutic antibody using structure-based computational design. Protein Sci. *15*, 949–960.

Dawson, J.P., Berger, M.B., Lin, C.C., Schlessinger, J., Lemmon, M.A., and Ferguson, K.M. (2005). Epidermal growth factor receptor dimerization and activation require ligand-induced conformational changes in the dimer interface. Mol. Cell. Biol. *25*, 7734–7742.

Dawson, J.P., Bu, Z., and Lemmon, M.A. (2007). Ligand-induced structural transitions in ErbB receptor extracellular domains. Structure *15*, 942–954.

de Haard, H.J., van Neer, N., Reurs, A., Hufton, S.E., Roovers, R.C., Henderikx, P., de Bruine, A.P., Arends, J.W., and Hoogenboom, H.R. (1999). A large non-immunized human Fab fragment phage library that permits rapid isolation and kinetic analysis of high affinity antibodies. J. Biol. Chem. *274*, 18218–18230.

DeLano, W.L. (2004). The PyMOL Molecular Graphics System (Palo Alto, CA: DeLano Scientific).

Emsley, P., and Cowtan, K. (2004). Coot: model-building tools for molecular graphics. Acta Crystallogr. D Biol. Crystallogr. *60*, 2126–2132.

Eswar, N., Webb, B., Marti-Renom, M.A., Madhusudhan, M.S., Eramian, D., Shen, M., Pieper, U., and Sali, A. (2006). Comparative protein structure modeling using MODELLER. In Current Protocols in Bioinformatics, A.D. Baxevanis, G.A. Petsko, L.D. Stein, and G.D. Stormo, eds. (New York: John Wiley & Sons), pp. 5.6.1–5.6.30.

Fellouse, F.A., Li, B., Compaan, D.M., Peden, A.A., Hymowitz, S.G., and Sidhu, S.S. (2005). Molecular recognition by a binary code. J. Mol. Biol. *348*, 1153–1162.

Ferguson, K.M. (2004). Active and inactive conformations of the epidermal growth factor receptor. Biochem. Soc. Trans. *32*, 742–745.

Ferguson, K.M., Darling, P.J., Mohan, M.J., Macatee, T.L., and Lemmon, M.A. (2000). Extracellular domains drive homo- but not hetero-dimerization of erbB receptors. EMBO J. *19*, 4632–4643.

Ferguson, K.M., Berger, M.B., Mendrola, J.M., Cho, H.S., Leahy, D.J., and Lemmon, M.A. (2003). EGF activates its receptor by removing interactions that autoinhibit ectodomain dimerization. Mol. Cell *11*, 507–517.

Franklin, M.C., Carey, K.D., Vajdos, F.F., Leahy, D.J., de Vos, A.M., and Sliwkowski, M.X. (2004). Insights into ErbB signaling from the structure of the ErbB2-pertuzumab complex. Cancer Cell *5*, 317–328.

French, A.R., Tadaki, D.K., Niyogi, S.K., and Lauffenburger, D.A. (1995). Intracellular trafficking of epidermal growth factor family ligands is directly influenced by the pH sensitivity of the receptor/ligand interaction. J. Biol. Chem. *270*, 4334–4340.

Garrett, T.P., McKern, N.M., Lou, M., Elleman, T.C., Adams, T.E., Lovrecz, G.O., Zhu, H.J., Walker, F., Frenkel, M.J., Hoyne, P.A., et al. (2002). Crystal structure of a truncated epidermal growth factor receptor extracellular domain bound to transforming growth factor α. Cell *110*, 763–773.

Garrett, T.P., McKern, N.M., Lou, M., Elleman, T.C., Adams, T.E., Lovrecz, G.O., Kofler, M., Jorissen, R.N., Nice, E.C., Burgess, A.W., et al. (2003). The crystal structure of a truncated ErbB2 ectodomain reveals an active conformation, poised to interact with other ErbB receptors. Mol. Cell *11*, 495–505.

Johns, T.G., Adams, T.E., Cochran, J.R., Hall, N.E., Hoyne, P.A., Olsen, M.J., Kim, Y.S., Rothacker, J., Nice, E.C., Walker, F., et al. (2004). Identification of the epitope for the epidermal growth factor receptor-specific monoclonal antibody 806 reveals that it preferentially recognizes an untethered form of the receptor. J. Biol. Chem. *279*, 30375–30384.

Jones, T.A., Zou, J.Y., Cowan, S.W., and Kjeldgaard, M. (1991). Improved methods for building protein models in electron density maps and the location of errors in these models. Acta Crystallogr. A *47*, 110–119.

Kohda, D., Odaka, M., Lax, I., Kawasaki, H., Suzuki, K., Ullrich, A., Schlessinger, J., and Inagaki, F. (1993). A 40-kDa epidermal growth factor/transforming growth factor α-binding domain produced by limited proteolysis of the extracellular domain of the epidermal growth factor receptor. J. Biol. Chem. *268*, 1976–1981.

Kuenen, B., Witteveen, E., Ruijter, R., Ervin-Haynes, A., Tjin-A-ton, M., Fox, F., Ding, C., Giaccone, G., and Voest, E.E. (2006). A phase I study of IMC-11F8, a fully human anti-epidermal growth factor receptor (EGFR) IgG1 monoclonal antibody in patients with solid tumors. Interim results. J. Clin. Oncol. *24*, 3024.

Lawrence, M.C., and Colman, P.M. (1993). Shape complementarity at protein/protein interfaces. J. Mol. Biol. *234*, 946–950.

Lemmon, M.A., Bu, Z., Ladbury, J.E., Zhou, M., Pinchasi, D., Lax, I., Engelman, D.M., and Schlessinger, J. (1997). Two EGF molecules contribute additively to stabilization of the EGFR dimer. EMBO J. *16*, 281–294.

Lenz, H.J. (2007). Management and preparedness for infusion and hypersensitivity reactions. Oncologist *12*, 601–609.

Li, S., Schmitz, K.R., Jeffrey, P.D., Wiltzius, J.J., Kussie, P., and Ferguson, K.M. (2005). Structural basis for inhibition of the epidermal growth factor receptor by cetuximab. Cancer Cell *7*, 301–311.

Liu, M., Zhang, H., Jimenez, X., Ludwig, D.L., Witte, L., Bohlen, P., Hicklin, D.J., and Zhu, Z. (2004). Identification and characterization of a fully human antibody directed against epidermal growth factor receptor for cancer therapy. AACR Meeting Abstracts *2004*, 163-c.

Lu, D., Jimenez, X., Witte, L., and Zhu, Z. (2004a). The effect of variable domain orientation and arrangement on the antigen-binding activity of a recombinant human bispecific diabody. Biochem. Biophys. Res. Commun. *318*, 507–513.

Lu, D., Zhang, H., Ludwig, D., Persaud, A., Jimenez, X., Burtrum, D., Balderes, P., Liu, M., Bohlen, P., Witte, L., et al. (2004b). Simultaneous blockade of both the epidermal growth factor receptor and the insulin-like growth factor receptor signaling pathways in cancer cells with a fully human recombinant bispecific antibody. J. Biol. Chem. *279*, 2856–2865.

Lu, D., Zhang, H., Koo, H., Tonra, J., Balderes, P., Prewett, M., Corcoran, E., Mangalampalli, V., Bassi, R., Anselma, D., et al. (2005). A fully human recombinant IgG-like bispecific antibody to both the epidermal growth factor receptor and the insulin-like growth factor receptor for enhanced antitumor activity. J. Biol. Chem. *280*, 19665–19672.

Marshall, J. (2006). Clinical implications of the mechanism of epidermal growth factor receptor inhibitors. Cancer *107*, 1207–1218.

McCoy, A.J. (2007). Solving structures of protein complexes by molecular replacement with Phaser. Acta Crystallogr. D Biol. Crystallogr. *63*, 32–41.

Nunez, M., Mayo, K.H., Starbuck, C., and Lauffenburger, D. (1993). pH sensitivity of epidermal growth factor receptor complexes. J. Cell. Biochem. *51*, 312–321.

Ogiso, H., Ishitani, R., Nureki, O., Fukai, S., Yamanaka, M., Kim, J.H., Saito, K., Sakamoto, A., Inoue, M., Shirouzu, M., et al. (2002). Crystal structure of the complex of human epidermal growth factor and receptor extracellular domains. Cell *110*, 775–787.

Otwinowski, Z., and Minor, W. (1997). Processing of X-ray diffraction data collected in oscillation mode. In Macromolecular Crystallography, C.W. Carter, Jr. and R.M. Sweet, eds. (New York: Academic Press), pp. 307–326.

Prewett, M., Tonra, J.R., Rajiv, B., Hooper, A.T., Makhoul, G., Finnerty, B., Witte, L., Bohlen, P., Zhu, Z., and Hicklin, D.J. (2004). Antitumor activity of a novel, human anti-epidermal growth factor receptor (EGFR) monoclonal antibody (IMC-11F8) in human tumor xenograft models. AACR Meeting Abstracts *2004*, 1235.

Scaltriti, M., and Baselga, J. (2006). The epidermal growth factor receptor pathway: a model for targeted therapy. Clin. Cancer Res. *12*, 5268–5272.

Schlessinger, J. (2000). Cell signaling by receptor tyrosine kinases. Cell *103*, 211–225.

Stanfield, R.L., Zemla, A., Wilson, I.A., and Rupp, B. (2006). Antibody elbow angles are influenced by their light chain class. J. Mol. Biol. *357*, 1566–1574.

Sunada, H., Magun, B.E., Mendelsohn, J., and MacLeod, C.L. (1986). Monoclonal antibody against epidermal growth factor receptor is internalized without stimulating receptor phosphorylation. Proc. Natl. Acad. Sci. USA *83*, 3825–3829.

Todaro, G.J., De Larco, J.E., and Cohen, S. (1976). Transformation by murine and feline sarcoma viruses specifically blocks binding of epidermal growth factor to cells. Nature *264*, 26–31.

Vagin, A., and Teplyakov, A. (1997). MOLREP: an automated program for molecular replacement. J. Appl. Crystallogr. *30*, 1022–1025.

Waterman, H., Sabanai, I., Geiger, B., and Yarden, Y. (1998). Alternative intracellular routing of ErbB receptors may determine signaling potency. J. Biol. Chem. *273*, 13819–13827.

Weiner, L.M. (2006). Fully human therapeutic monoclonal antibodies. J. Immunother. *29*, 1–9.

Zhang, X., Gureasko, J., Shen, K., Cole, P.A., and Kuriyan, J. (2006). An allosteric mechanism for activation of the kinase domain of epidermal growth factor receptor. Cell *125*, 1137–1149.

Zhen, Y., Caprioli, R.M., and Staros, J.V. (2003). Characterization of glycosylation sites of the epidermal growth factor receptor. Biochemistry *42*, 5478–5492.

Accession Numbers

Coordinates have been deposited in the RCSB Protein Data Bank under ID codes 3B2U (Fab11F8/sEGFRd3) and 3B2V (Fab11F8/sEGFR).